

Hydroxyapatite for biomedical applications: A short overview

*Original*

Hydroxyapatite for biomedical applications: A short overview / Fiume, E.; Magnaterra, G.; Rahdar, A.; Verne', E.; Baino, F.. - In: CERAMICS. - ISSN 2571-6131. - ELETTRONICO. - 4:4(2021), pp. 542-563. [10.3390/ceramics4040039]

*Availability:*

This version is available at: 11583/2937032 since: 2021-11-11T10:46:17Z

*Publisher:*

MDPI

*Published*

DOI:10.3390/ceramics4040039

*Terms of use:*

openAccess


This article is made available under terms and conditions as specified in the corresponding bibliographic description in the repository

*Publisher copyright*

(Article begins on next page)

Review

# Hydroxyapatite for Biomedical Applications: A Short Overview

Elisa Fiume <sup>1</sup>, Giulia Magnaterra <sup>1</sup>, Abbas Rahdar <sup>2</sup>, Enrica Verné <sup>1</sup> and Francesco Baino <sup>1,\*</sup>

<sup>1</sup> Department of Applied Science and Technology (DISAT), Institute of Materials Physics and Engineering, Politecnico di Torino, 10129 Turin, Italy; elisa.fiume@polito.it (E.F.); mgiulia.94@hotmail.it (G.M.); enrica.verne@polito.it (E.V.)

<sup>2</sup> Department of Physics, University of Zabol, Zabol 98613-35856, Iran; a.rahdar@uoz.ac.ir

\* Correspondence: francesco.baino@polito.it

**Abstract:** Calcium phosphates (CaPs) are biocompatible and biodegradable materials showing a great promise in bone regeneration as good alternative to the use of auto- and allografts to guide and support tissue regeneration in critically-sized bone defects. This can be certainly attributed to their similarity to the mineral phase of natural bone. Among CaPs, hydroxyapatite (HA) deserves a special attention as it, actually is the main inorganic component of bone tissue. This review offers a comprehensive overview of past and current trends in the use of HA as grafting material, with a focus on manufacturing strategies and their effect on the mechanical properties of the final products. Recent advances in materials processing allowed the production of HA-based grafts in different forms, thus meeting the requirements for a range of clinical applications and achieving enthusiastic results both in vitro and in vivo. Furthermore, the growing interest in the optimization of three-dimensional (3D) porous grafts, mimicking the trabecular architecture of human bone, has opened up new challenges in the development of bone-like scaffolds showing suitable mechanical performances for potential use in load bearing anatomical sites.



**Citation:** Fiume, E.; Magnaterra, G.; Rahdar, A.; Verné, E.; Baino, F. Hydroxyapatite for Biomedical Applications: A Short Overview. *Ceramics* **2021**, *4*, 542–563. <https://doi.org/10.3390/ceramics4040039>

Academic Editors: Anna Lukowiak and Gilbert Fantozzi

Received: 30 June 2021

Accepted: 24 September 2021

Published: 28 September 2021

**Publisher's Note:** MDPI stays neutral with regard to jurisdictional claims in published maps and institutional affiliations.



**Copyright:** © 2021 by the authors. Licensee MDPI, Basel, Switzerland. This article is an open access article distributed under the terms and conditions of the Creative Commons Attribution (CC BY) license (<https://creativecommons.org/licenses/by/4.0/>).

**Keywords:** bioceramics; calcium phosphate; hydroxyapatite; bone; tissue engineering

## 1. Introduction

Since the early 1900s, the scientific community began to be interested in calcium phosphates (CaPs) as materials for the production of bone substitutes in biomedical applications. The first study dates back to 1920, when CaPs were used as filler material to repair critical size bone defects in rabbits [1].

Owing to their physico-mechanical properties, which are similar to those of human bone, as well as osteogenic potential both in vivo and in vitro [2]. Today CaPs are widely used in different fields of medicine, such as otolaryngology, skull and maxillofacial reconstruction, spinal surgery, orthopedics, treatment of osseous fractures and bone disorders, percutaneous implants and dentistry/periodontal surgery [3]. A study conducted in the USA showed that in 2010 about 1.3 billion dollars were invested in CaP-based bone substitutes only [4].

The term “CaPs” refers to a family of minerals containing calcium cations ( $\text{Ca}^{2+}$ ) and metaphosphate ( $\text{PO}^{-}_3$ ), orthophosphate ( $\text{PO}_4^{3-}$ ), or pyrophosphate ( $\text{P}_2\text{O}_7^{4-}$ ) anions [3], as well as hydroxyl ( $\text{OH}^-$ ) or hydrogen ( $\text{H}^+$ ) ions [5].

CaPs are the main constituents of tooth enamel (~90 wt.%) and bone (~60 wt.%) [5], and this is the main reason why they are studied in bone repair and regeneration.

They exhibit crystalline structure and chemical properties very similar to those of bone apatite [6] and excellent biocompatibility with living cells [7,8].

CaPs are well known to have osteoconductive properties that permit the attachment, proliferation and migration of bone cells, regardless of the form in which they are used (e.g., coating, powder, bulk or porous scaffolds). Soluble and/or nano-sized CaPs were also reported to exhibit osteoinductive properties, thus actively promoting the growth and regeneration of new bone [9,10].

During their permanence into the human body, most of CaPs can be partially dissolved within body fluids. The local increment in  $\text{Ca}^{2+}$  and  $\text{PO}_4^{3-}$  ions at the bone/implant interface determines the supersaturation of the biological environment and the consequent precipitation of apatite nanocrystals on the material surface [11]. This newly-formed layer can adsorb proteins from the surrounding environment, thus promoting the attachment, proliferation and differentiation of osteoprogenitor stem cells and the consequent mineralization of the tissue and the formation of osteoids. The angiogenesis progression will finally result in local bone induction and potential incorporation of the CaP implant within the natural bone [11].

The rate of formation of the surface apatite layer depends on the type of bioceramic considered; it takes 30 days for hydroxyapatite, and about 14 days for  $\beta$ -tricalcium phosphate [12]. For the purpose of comparison, bioactive glasses, which have a faster reactivity in contact with biological fluids, are able to form a surface apatite layer in the range of few hours to few days [13].

The distinction between osteoconductive and osteoinductive biomaterials is obviously dictated also by the time scale of reactivity *in vitro* and *in vivo*; this is the reason why highly-reactive materials such as bioactive glasses or soluble CaPs are classified as belonging to the latter group, while non-porous hydroxyapatite, which has an almost negligible solubility, is a traditional example of the former [14].

Qui and Ducheyne have described the general reactions occurring at the interface between CaPs and biological environment through a 11-step sequence [11]:

1. Dissolution of CaPs;
2. Precipitation from the solution on the surface of CaPs;
3. Ion transfer and structural adjustment at the tissue/CaP interface;
4. Dispersion from the boundary surface layer in the CaPs;
5. Effects mediated by the solution on cell activity;
6. Organic and mineral phase deposition without integration into the CaP surface;
7. Deposition with integration of CaPs into the surface;
8. Chemotaxis to the surface of CaPs;
9. Cells attachment and proliferation;
10. Differentiation of cells;
11. ECM formation.

CaPs are also good vehicles for bioactive peptides, growth factors and various cell types [4]. They are helpful in mesenchymal stem cell differentiation and influence the expression of osteoblastic differentiation markers such as alkaline phosphatase (ALP), bone morphogenetic proteins (BMPs) and collagen type I (COL1) [3].

The intrinsic micropores of CaP materials produced by sintering of powders can have a filtering effect and store the growth factors from the surrounding fluids [15].

Osteoinduction is strongly influenced not only by porosity, which can accelerate solubility and promote interactions with cells and biomolecules, but also by other parameters such as composition, degree of crystallinity (high crystallinity indicates low degradation rates) and, in general, surface area (e.g., granular product vs. bulk blocks) [16].

Typically, higher degradation rates lead to a better osteoinductive potential [11].

Sometimes the osteoinductivity of CaPs can be increased by adding particular osteoinductive signaling molecules (extrinsic osteoinductivity) or by performing a chemical and/or structural optimization of the material itself (intrinsic osteoinductivity) [17].

The various types of CaPs differ for their specific Ca/P ratio, which involves a different release of calcium and phosphate ions that will play a key role in bone mineralization [3,6,18].

The chemical stability of CaPs in terms of dissolution rate is influenced by pH changes and can be designed at the material's synthesis stage by acting on the temperature, type of solvent, pressure and kind of precursors used [19].

A "technological" strategy to control dissolution relies on modulating the available surface area by changing the sintering temperature. By decreasing the sintering tempera-

ture of CaPs, the residual inter-particle microporosity will increase and, consequently, the specific surface area will increase too. In contrast, by raising the sintering temperature, the size of the micropores decreases as well as their volume, leading to a decrease in the specific surface area [11].

Despite the crystallographic similarity with the mineral phase of bone, CaPs suffer from some limitations including the lack of an organic phase (e.g., collagen), which can be partially mitigated by the development of composites [20], low mechanical strength and high brittleness, which make them unsuitable for load-bearing prosthetic applications, in which tougher metallic implant are typically preferred.

For dense bioceramics, the strength is a function of the grain size: the smaller the crystals, the more resistant the ceramic. Moreover, the mechanical properties increase as the crystalline phase increases and porosity decreases. If the crystalline phase is predominant over the amorphous fraction, CaPs will be characterized by greater compressive and tensile strength and fracture toughness [4,10].

It was estimated that, in order to achieve maximum packing and minimum shrinkage after sintering—and hence higher mechanical strength—it is advisable to use a percentage of coarse powders equal to 70% of the total, with the remaining 30% of fine powders [4].

In summary, CaPs are brittle polycrystalline materials with mechanical properties related to solubility in vitro and in vivo, which strictly depend on the composition, crystallinity, grain size and porosity. A strategy to finely modulate the mechanical properties of CaPs relies on producing multiphasic CaP compounds. This approach involves the preparation of homogeneous mixtures of two (biphasic), three (triphasic) or more (multiphasic) single phases of CaPs with different solubility [7].

Table 1 shows the main CaPs used in biomedical applications and their major characteristics. As regards the most commonly-used CaPs, the solubility and dissolution rate follow this trend:  $\alpha$ -TCP >  $\beta$ -TCP > HA > FA.

**Table 1.** Existing CaPs and their major properties, adapted from [4].

Material	Chemical Formula	Ca/P Molar Ratio	Solubility at 25 °C, g/L	pH Stability Range in Aqueous Solutions (25 °C)
Monocalcium phosphate monohydrate (MCPM)	$\text{Ca}(\text{H}_2\text{PO}_4)_2 \cdot \text{H}_2\text{O}$	0.5	~18	0.0–2.0
Dicalcium phosphate dehydrate (DCPD), mineral brushite	$\text{CaHPO}_4 \cdot 2\text{H}_2\text{O}$	1.0	~0.088	2.0–6.0
Octacalcium phosphate (OCP)	$\text{Ca}_8(\text{HPO}_4)_2(\text{PO}_4)_4 \cdot 5\text{H}_2\text{O}$	1.33	~0.0081	5.5–7.0
$\alpha$ -Tricalcium phosphate ( $\alpha$ -TCP)	$\alpha\text{-Ca}_3(\text{PO}_4)_2$	1.5	~0.0025	a
$\beta$ -Tricalcium phosphate ( $\beta$ -TCP)	$\beta\text{-Ca}_3(\text{PO}_4)_2$	1.5	~0.0005	a
Amorphous calcium phosphate (ACP)	$\text{Ca}_x\text{H}_y(\text{PO}_4)_z \cdot n\text{H}_2\text{O}$ , $n = 3\text{--}4.5, 15\text{--}20\%$ $\text{H}_2\text{O}$	1.0–2.2 <sup>c</sup>	b	5.0–12.0
Hydroxyapatite (HA)	$\text{Ca}_{10}(\text{PO}_4)_6(\text{OH})_2$	1.67	~0.0003	9.5–12.0
Fluorapatite (FA)	$\text{Ca}_{10}(\text{PO}_4)_6\text{F}_2$	1.67	~0.0002	7.0–12.0
Oxyapatite (OA)	$\text{Ca}_{10}(\text{PO}_4)_6\text{O}$	1.67	~0.087	a
Tetracalcium phosphate (TTC)	$\text{Ca}_{10}(\text{PO}_4)_2\text{O}$	2.0	~0.0007	a

<sup>a</sup> These compounds cannot be precipitated from aqueous solutions. <sup>b</sup> The solubility of ACP cannot be measured precisely. However, the following values of  $\log(K_s)$  were found, as reported in [6]:  $25.7 \pm 0.1$  (pH = 7.40),  $29.9 \pm 0.1$  (pH = 6.00) and  $32.7 \pm 0.1$  (pH = 5.28). The comparative extent of dissolution in acidic buffer is:  $\text{ACP} \gg \alpha\text{-TCP} \gg \beta\text{-TCP} \gg \text{HA} > \text{FA}$  [6]. <sup>c</sup> A Ca/P ratio lower than 1 was reported under special experimental conditions [18].

CaPs are mainly used in tissue engineering in the form of granules and micro-particles, cements and injectable pastes, coatings and scaffolds [5]. More recently, they have started being used to create nano-sized systems (e.g., nano-tubes or nano-needles) [21] or in the form of dispersed nanoparticles.

Injectable CaPs (e.g., water-based pastes) can be easily transported through a non-invasive method to the defect site, where they subsequently harden, repair the defect and support the regeneration of new tissue over time. This also allows them to be used as a drug delivery system or to treat a defect in difficult areas, such as the craniofacial complex or the spine (vertebroplasty) [16]. A good overview of commercial products used in clinics is reported by Islam et al. [16].

Among the many existing CaPs, undoubtedly hydroxyapatite (HA) and tricalcium phosphate (TCP) play a very important role in the development of bone tissue engineering (BTE) products [8,9]. TCP is an osteoconductive material and supports the formation of new bone through the release of calcium and phosphate ions; it also degrades quickly upon contact with human body fluids. HA, as already pointed out, is known for its biocompatibility and high osteoconductivity, together with a higher chemical stability in contact with body fluids than TCP [22]. Thanks to these properties, HA has been and still is among the most studied and used materials in the field of BTE [8] and, given its relevance in medicine, will be the topic of the present review.

## 2. Chemical Structure of HA and Its Properties

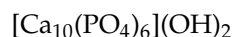
The term “apatite” derives from the Greek for “*apatáo*” meaning “I am mistaken” as, in the past, it has been often confused with several other minerals such as fluorite and beryl. It was first used by Werner in 1786, and includes a family of compounds with similar structure (hexagonal system, space group P63/m); however, the exact structure of apatites may change due to the different types of morphologies and non-stoichiometric variations that exist.

The general formula for apatite is:



where M = bivalent cation and Z = monovalent anion.

The specific name and properties of each apatitic compound depend on M and Z. As regards HA, the bivalent cation (M) corresponds to  $Ca^{2+}$  and Z to the hydroxyl radical ( $OH^-$ ); hence, the chemical formula of HA is:



As displayed in Figure 1, HA exhibits a rather complex crystalline structure consisting of phosphate ions ( $PO_4^{3-}$ ), hydroxyl ions ( $OH^-$ ) and calcium ions ( $Ca^{2+}$ ), and there are two formula units in the cell of the crystallographic unit [23]. The amounts of calcium, phosphate and hydroxyl ions are 39.84, 56.77 and 3.39 wt.%, respectively.

The unit cell has a hexagonal-like structure with space group P63/m, cell parameters  $a = b = 9.4225 \text{ \AA}$  and  $c = 6.8850 \text{ \AA}$  and direction of crystal growth along the c-axis [2,24].

In comparison with other CaP ceramics, HA is stable in an aqueous environment over a pH range of 4.2 to 8.0 [25].

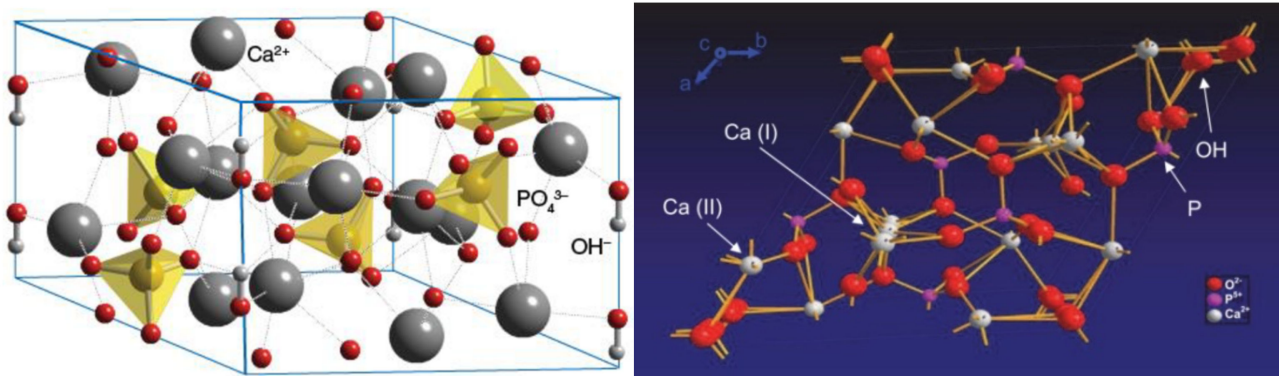


Figure 1. The crystalline structure of HA [5].

In each unit cell, the calcium ions can occupy two sites labelled as I and II, and the  $\text{PO}_4^{3-}$  ions are divided into two planes at a crystal height of  $\frac{1}{4}$  and  $\frac{3}{4}$ , respectively, yielding the creation of two different types of channels across the  $c$  axis named channel A and channel B [26]. In channel A, there are oxygen atoms of the phosphate group and ions of calcium type II (Ca(II)) arranged at the vertices of two equilateral triangles that are rotated of  $60^\circ$  from each other. The type B channel, with a diameter of  $2 \text{ \AA}$ , contains type I calcium ions (Ca(I)) only.

Each unit cell comprises/share:

- 14  $\text{Ca}^{2+}$  ions: 6 of them inside the cell, and 8 shared with adjacent cells; total = 10  $\text{Ca}^{2+}$  ions/unit cell
- 10  $\text{PO}_4^{3-}$  ions: 2 of them located inside the cell, and 8 peripheral ions shared with as many adjacent cells; total = 6  $\text{PO}_4^{3-}$  ions/unit cell
- 8  $\text{OH}^-$  ions: being along the edges, they all belong to the cell by  $\frac{1}{4}$ ; total = 2  $\text{OH}^-$  ions/unit cell (see Figure 2).

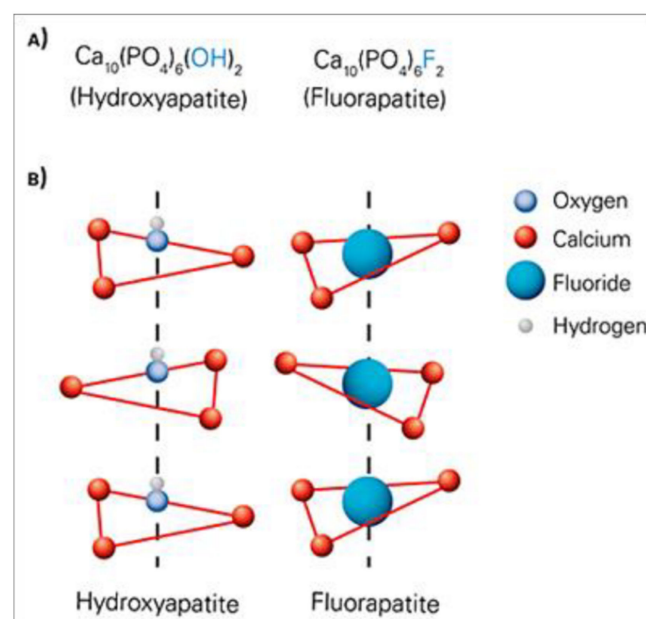


Figure 2. Comparison between the chemical formula (A) and structure (B) of HA and FA (courtesy of Enrica Verné).



Due to a different distribution of  $\text{OH}^-$  ions, it is possible to distinguish two types of HA: stoichiometric HA (or hexagonal HA) and monoclinic HA. In the stoichiometric HA, there are  $\text{OH}^-$  radicals with alternate orientations at the center of type A channels.

Monoclinic HA is more thermodynamically stable and ordered than the hexagonal one; it forms at high temperatures and there is no evidence of its presence in calcified tissues.

The crystalline structure of HA can accommodate substitutions by various other ions for the  $\text{Ca}^{2+}$ ,  $\text{PO}_4^{3-}$  and  $\text{OH}^-$  groups. Ionic replacements can affect crystal morphology, crystallinity, solubility, lattice parameters, thermal stability and biological response of HA. Cationic substitutions occur at sites that are normally occupied by calcium atoms, whereas anionic substitutions may involve either phosphates or hydroxyl ions. Chlorapatite and fluorapatite are common examples of anion-substituted HA, where  $\text{OH}^-$  ions are replaced by  $\text{Cl}^-$  and  $\text{F}^-$  ions, respectively (Figure 2).

Substitution of hydroxyl or phosphate ions with  $\text{CO}_3^{2-}$  ions leads to the formation of carbonate apatite that, although being classifiable as a bone apatite, cannot be used directly for osseous repair as it would induce inflammatory response upon implantation. Carbonate apatite is typically used after being sintered so that it partially decomposes at high temperature. Doy et al. [27] reported that specimens of carbonate apatite with 12 wt.% of carbonate content could be sintered at 600–750 °C and retained around 6 wt.% of carbonate substitution in the lattice, which was comparable to that of bone apatite. In general, the reactivity of carbonate apatite in body fluids is higher than that of HA, thus yielding to fat dissolution rates depending on pH and particle/granule size [28].

HA is characterized by a Ca/P atomic ratio of 1.67, similar to that of biological apatite in human bones and teeth, thus making it very suitable for orthopedic, dental and maxillofacial repair [29,30].

In general, the closer the Ca/P value to 1.67, the greater the stability of HA inside the human body [26].

Ca-deficient HAs with Ca/P < 1.67 exhibit a certain degree of solubility; they may form, for example, as transient CaPs on the surface of bioactive glasses in vitro but then tend to evolve to stoichiometric HA during the bioactivity process [31–33].

It has also been shown that the mechanical strength of CaPs increases with increasing Ca/P ratio and reaches its maximum value if the Ca/P ratio is ~1.67 (stoichiometric HA), while it decreases suddenly if the Ca/P ratio exceeds 1.67 [4]. Furthermore, by altering the Ca/P molar ratio, it is possible to finely design the dissolution rate of CaPs [2].

Table 2 summarizes the principal properties of HA [5].

**Table 2.** Principal properties of HA [5].

Property	Value	Property	Value
Density	3.16 g/cm <sup>3</sup>	Poisson's ratio	0.27
Decomposition temperature	>1000 °C	Fracture Energy	2.3–20 J/m <sup>2</sup>
Dielectric constant	7.40–10.47	Fracture toughness	0.7–1.2 MPa·m <sup>1/2</sup> (decrease with porosity)
Thermal conductivity	0.013 W/cm·K	Fracture hardness	3–7 GPa (dense HA)
Melting point	1614 °C	Biocompatibility	High
Tensile strength	38–300 MPa (dense HA) ~3 MPa (porous HA)	Biodegradation	Low
Bending strength	38–250 MPa (dense HA) 2–11 MPa (porous HA)	Bioactivity	High
Compressive strength	120–900 MPa (dense HA) 2–100 MPa (porous HA)	Osteoconduction	High
Young's elastic modulus	35–120 GPa	Osteoinduction	Nil

In addition to the composition, the shape, size and distribution of HA crystals also significantly affect the mechanical, biochemical and biological properties the material [34,35]. In turn, these characteristics are dependent on the technique used for making HA powders.

### 3. HA Synthesis Techniques

The synthesis techniques for producing man-made HA can be divided into four main groups, which are briefly described in the following sections.

The most commonly-used synthesis routes are also summarized in Table 3; the interested Reader can find more details elsewhere [35].

**Table 3.** Major processing techniques for producing HA powders along with relevant properties; adapted from [36].

Processing Technique	Typical Procedure	Powder Property
Solid-state synthesis	Calcium and phosphate containing compounds. Sintering ~ 1250 °C	HA particles with heterogeneous size (from nano- to micro-scale) and shape.
Mechanochemical method	Slow mixing of Ca(OH) + H <sub>3</sub> PO <sub>4</sub> / (CH <sub>3</sub> COO) <sub>2</sub> Ca + KH <sub>2</sub> PO <sub>4</sub> / Ca(NO <sub>3</sub> ) <sub>2</sub> + (NH <sub>4</sub> ) <sub>2</sub> HPO <sub>4</sub> solutions using vigorous stirring, followed by aging	HA nanoparticles of 50–100 nm length. HA nanorods of 50 nm diameter. HA nanospheres of 200 nm size
Hydrothermal method	Hydrothermal treatment of an aqueous mixture of pH 4.5 comprising Ca(NO <sub>3</sub> ) <sub>2</sub> , NaH <sub>2</sub> PO <sub>4</sub> , HNO <sub>3</sub> and urea at 160 °C for about 3 h	HA whiskers of 10 µm width and 150 µm length
Sol-gel method	Aging an ethanol solution of pH 10 comprising Ca(NO <sub>3</sub> ) <sub>2</sub> , (NaH) <sub>2</sub> PO <sub>4</sub> , NH <sub>4</sub> OH, and PEG at 85 °C for 4 h, followed by drying	Sintered HA nanocrystals of 50–70 nm size
Sonochemical method	Ultrasonic irradiation (28–34 kHz, 100 W) of a pseudo-body solution containing NaCl, KCl, NaH <sub>2</sub> PO <sub>4</sub> , KH <sub>2</sub> PO <sub>4</sub> , CaCl <sub>2</sub> and MgCl <sub>2</sub>	Spherical HA nanoparticles of 18 nm size with a specific surface area up to
Synthesis method based on biogenic sources	Thermal treatment of deproteinized bovine bone, then crushing and ball milling, followed by vibro-milling using ethanol	Needle-like HA nanopowder of ~100 nm size

#### 3.1. Dry Methods

Dry methods include two different approaches: solid-state synthesis and mechanochemical method. HA powders made using dry methods are usually characterized by a large grain size and an irregular shape [35], which often derive from using low-cost raw material [37]. The size of the particles is usually above the nano-scale and their phase purity is lower as compared to wet methods [37].

According to the literature, dry methods do not require any particular processing conditions and do not use a solvent [35].

Solid-state synthesis is a relatively simple procedure and is particularly advisable for mass-production of HA particles. Usually, a previously prepared CaP salt is used as a



precursor, which is then ground and calcined at high temperature (e.g., 1000 °C). The high calcination temperature leads to the formation of a good crystalline structure. The final particles are heterogeneous and rather irregularly shaped.

The second strategy, known as mechano-chemical method or mechanical alloying, allows obtaining a powder with a much more defined structure as compared to the solid-state method, owing to perturbation of surface-bonded species as a result of pressure, which improves kinetic and thermodynamic reactions between solids [35]. In a typical process, the materials are ground by using a planetary mill and the molar ratio between the reagents is kept at the stoichiometric ratio. This technique is relatively simple and easily reproducible [35]; the principal processing variables are the type of reagents, the type of milling medium, the rotational speed and the duration of working phases and interval steps [35]. During their experiments, Nasiri-Tabrizi et al. [38] have proven that the average size of powder decrease with the increase of milling time; this also yields an increase of lattice strain.

The high reproducibility combined with low processing costs make dry methods the most suitable ones for the production of HA micro-particles in large amounts [34].

### 3.2. Wet Methods

Unlike dry methods, wet methods allow obtaining HA nanoparticles with a regular morphology. For this reason, they are the most widely-used methods for the synthesis of nano-powders [39].

One of the main disadvantages of wet methods is the low temperature used during preparation, which leads to the formation of CaP phases other than HA and/or traces of impurities in the crystalline structure due to ions from the aqueous solution used for the synthesis [35].

These methods can be divided into six subgroups, i.e., conventional chemical precipitation, hydrolysis, sol-gel, hydrothermal method, emulsion method and sono-chemical method.

Chemical precipitation represents one of the easiest wet methods used for HA powder preparation. It is based on the fact that, at pH 4.2 and room temperature, HA is usually stable and not very soluble in an aqueous solution; however, the precipitation reaction is usually conducted at pH > 4.2 [35]. For this technique, CaP-containing precursors such as calcium nitrate or calcium hydroxide and diammonium hydrogen phosphate or orthophosphoric acid [35] are typically used. Usually, the reagents should be added drop-by-drop, under mild conditions and continuous stirring, checking that the molar Ca/P ratio remains at approximately 1.67. Then the suspension, after being carefully filtered and dried, is either aged for a period at atmospheric pressure or immediately reduced to powder [35]. HA particles produced by this method are, however, non-stoichiometric and poorly crystalline [19]. In order to obtain powders with higher phase purity, the precipitation reaction must be conducted at higher temperature or higher pH or both; in this way, the risk of formation of phase impurities decreases as well [35].

Hydrolysis method involves the preparation of HA nanoparticles by hydrolysis of other CaP phases, such as dicalcium phosphate dihydrate (DCPD), tricalcium phosphate (TCP) under certain conditions and, also, octacalcium phosphate (OCP). To date, OCP has almost completely been abandoned since it tends to incorporate impurities during its transformation into HA [35]. Tenhuisen et al. [40] reported the production of HA from TCP and observed a linear relationship between the hydrolysis temperature and the resulting surface area of HA. It was also noted that, by increasing the reaction temperature, the regularity of the crystals increases [35]. Park et al. [41] have demonstrated that the aspect ratio, thermal stability and stoichiometry of HA strongly depend on the pH during hydrolysis.

Sol-gel method allows obtaining fine and homogeneous powders thanks to the mixing of the reagents at molecular level and the possibility of using a low processing temperature [35]. The relevant reactions lead to the formation of a solid gel from a colloidal

solution (liquid sol). The starting materials for the preparation of sols usually include inorganic salts or salts of organic acids or alkoxides [35]. The precursors undergo a series of hydrolysis and polymerization reactions to form a colloidal suspension (the sol) that, spontaneously over time and/or under the action of temperature or a catalyst, transforms to a gel. The gel is then aged at room temperature, dried and, finally, calcined at high temperature in order to eliminate the organic residues [35]. The main steps of the sol-gel method are shown in Figure 3. A long aging period is necessary for the formation of HA as the reaction between the calcium and phosphorus precursors (in solution) is very slow [35]. The nature of the solvent, the rate of gelation and the temperature and pH chosen for the process strongly depend on the type of precursors used. In vitro studies have shown that nano-sized HA made by the sol-gel method has a bio-absorbability rate similar to that biological apatite [42]. HA powders prepared by the sol-gel method shows nano-structured primary particles that can agglomerate into micrometric grains (Figure 4). The major disadvantages of this method include the high cost of the starting materials and the risk of generating CaO in the final product. Secondary CaO phase has been shown to be harmful to the biocompatibility, thus it is necessary to remove it either by properly adjusting the main procedure or by washing the powder with a dilute acid solution (e.g., HCl).

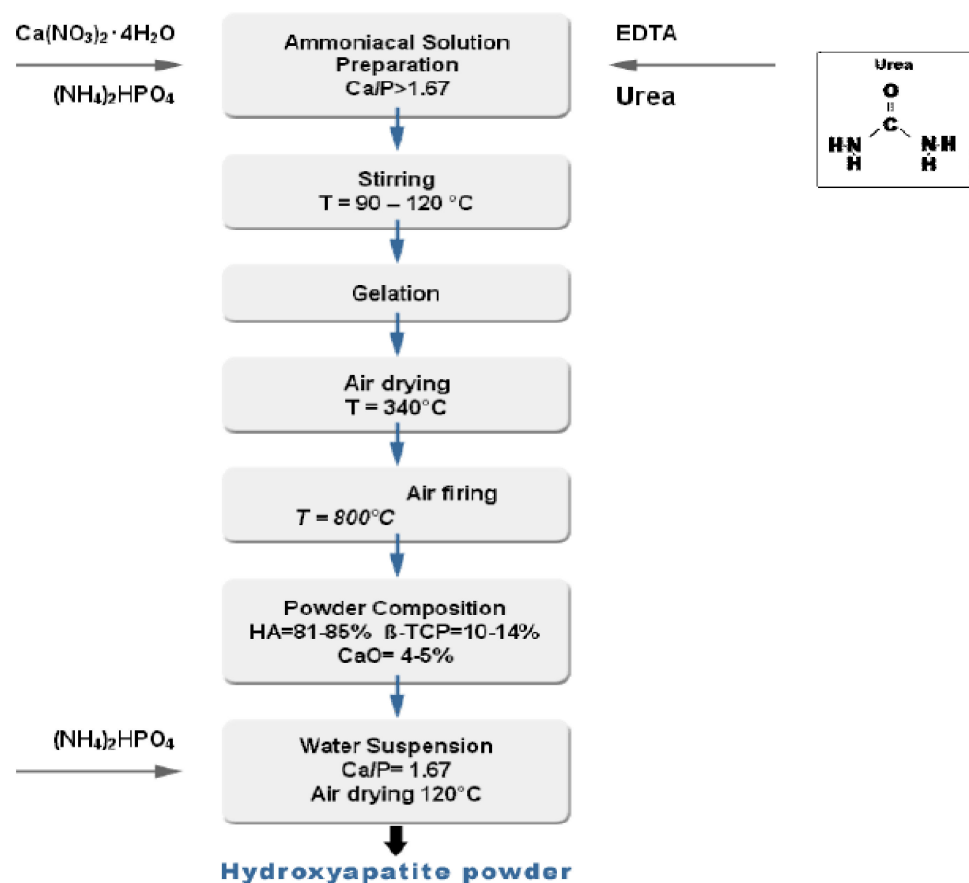
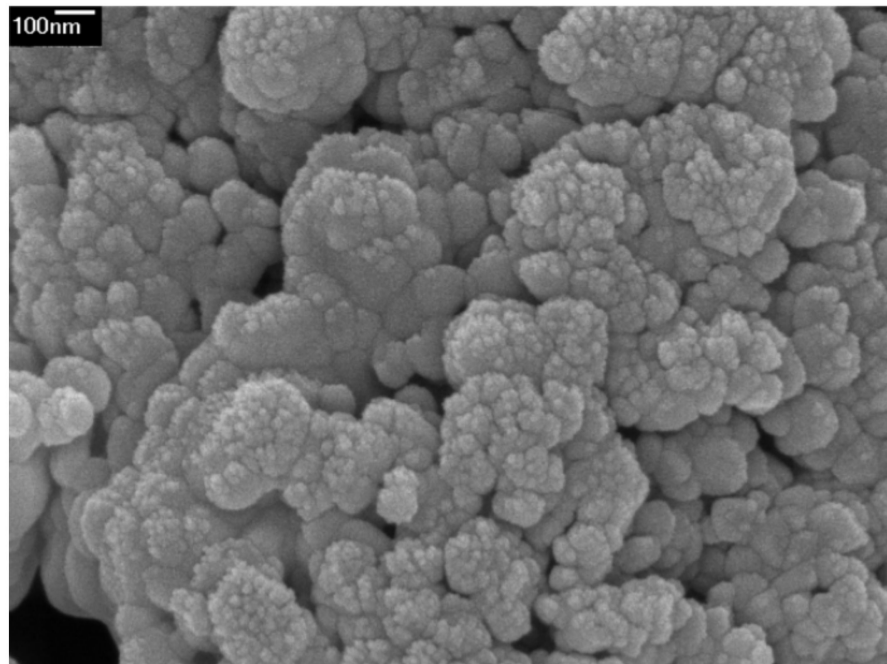


Figure 3. HA preparation scheme using sol-gel method (courtesy of Enrica Verné).



**Figure 4.** HA powder prepared via sol-gel [43].

Hydrothermal method is characterized by high working temperature and pressure. It can be considered as a chemical precipitation method in which the aging phase is conducted at high temperature [35]. The procedure is carried out in an autoclave, where the high temperature in a closed environment favors the formation of solvent vapor and a subsequent increase in pressure. Using a high-temperature results in a higher phase purity than that achievable by traditional sol-gel methods and a suitable Ca/P ratio. However, high temperatures and pressures require expensive equipment, making this process less affordable than other wet methods [35]. The hydrothermal method typically allows obtaining HA crystals with irregular morphology, at most spherical or rod-like; hexagonal prisms with 0.1  $\mu\text{m}$  length were obtained by strictly controlling temperature, pH and in the presence of ethylenediamine tetraacetic acid (EDTA) [44].

Emulsion method is one of the most effective strategies for reducing particle size and achieving a controlled morphology and fine structure by limiting particle agglomeration [35]. This technique was originally used to make porous materials [45]. The most common reagents are phosphoric acid and calcium nitrate because they are quite cheap and easy to be found on the market [44]. The most used surfactants are polyoxyethylene, cetyltrimethyl ammonium bromide and dioctyl sodium sulfosuccinate salt. It is a rather simple method and uses low processing temperatures and mild synthesis conditions [46–48].

Sonochemical method is based on chemical reactions activated by powerful ultrasonic waves. The physical mechanism behind the synthesis is acoustic cavitation in an aqueous phase. The reactivity of chemicals is stimulated to accelerate heterogeneous reactions between liquid and solid reagents. It has recently been demonstrated that HA particles synthesized with this process possess more uniform, smaller and purer crystals [35]. Hazar Yoruç and İpek [49] have proved that the HA particle size decreases significantly by increasing the ultrasonic power up to 300 W. Due to the high speed and high kinetic energy stored during the synthesis, it is more likely that HA particles can collide with each other and create a more uniform crystal lattice. This characteristic can improve mechanical properties of final product.

### 3.3. High-Temperature Processes

These processes are characterized by the need for using high temperatures to partially or completely burn the precursors [35]. There are two different methods based on combustion and pyrolysis.

Combustion method (Figure 5) allows quickly producing highly pure powder with a single operation. This approach has some important advantages in terms of relatively simple process execution, cheap raw materials and good chemical homogeneity of the synthesized powder as a result of intimate mixing of the components [35].

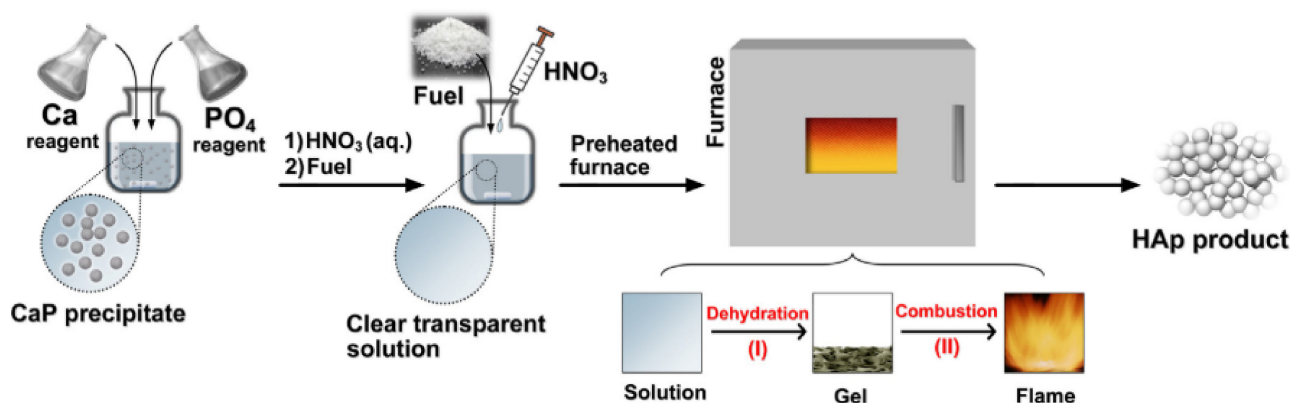


Figure 5. Preparation of HA nanoparticles via the solution combustion method [35].

The combustion of the HA solution causes an exothermic and self-sufficient redox reaction between an organic fuel (e.g., citric acid, succinic acid, glycine, urea and sucrose) and oxidants (e.g., calcium nitrate  $\text{Ca}(\text{NO}_3)_2$  or nitric acid ( $\text{HNO}_3$ )). As shown in Figure 5, the aqueous solutions of  $\text{Ca}(\text{NO}_3)_2$  and ammonium sulphate ( $(\text{NH}_4)_2\text{HPO}_4$ ) are initially mixed together; then,  $\text{HNO}_3$  is added to dissolve the obtained precipitate. A mixture of two fuels is then incorporated (sometimes even a single fuel is used) [35]. In order to start the reaction, the mixture is heated in an oven at a relatively low temperature (about 300 °C). Then, due to combustion, there is a sudden increase in temperature to a maximum. Finally, the mixture is cooled rapidly so that maximum nucleation is induced, and unwanted further growth of the particles is avoided. Exothermic combustion reaction provides sufficient heat to maintain the system temperature and avoid the need for external heating. There are many parameters that influence the maximum reaction temperature and, consequently, the characteristics of the final powder, such as fuel/oxidant ratio, initial furnace temperature and nature of the fuel. The resulting product is usually an agglomeration of very fine particles [35].

Pyrolysis is relatively simple and fast because it does not involve any post-treatments and/or long-term aging at high temperatures, but still guarantees the production of stoichiometric, homogeneous and highly-crystalline particles [35]. The pyrolysis method is also known as “pyrolysis spray” because the precursor solutions are sprayed inside a hot oven using an ultrasonic generator. This is followed by the reaction of the vapors and gases generated at high temperatures and the production of the final powder. The high temperature causes the complete evaporation of the precursors, followed by nucleation and growth of the nanoparticles in the gaseous phase. A disadvantage of this technique is the possible formation of secondary aggregations, with consequent decrease in the specific surface area.

### 3.4. Synthesis Method Based on Biogenic Sources or Bioinspired Approaches

HA obtained partially or entirely from biogenic sources integrate better within the human body due to a greater physico-chemical similarity with bone apatite [35]. HA can be extracted from fish scales or fish bones, bovine bones, eggshells or from the exoskeleton

of marine organisms. A period of annealing which lasts for several hours is generally required to obtain HA. In this way, the organic part of the bone is removed, and the pure HA particles remain.

Simple thermal annealing is not the only extraction process that can be used; the following are also possible: plasma processing, subcritical water processing, enzymatic hydrolysis and alkaline hydrothermal hydrolysis [35]. All these methods make it possible to remove organic substances from bone and produce pure HA with an average yield of 65%.

Several experiments have been conducted to try decreasing the particle size at the nanoscale by means of the vibro-milling method that was used, for example, by Ruksudjarit et al. [50] who obtained HA from bovine bone. The bovine bone was deproteinized in hot water and calcined at 800 °C, crushed into small pieces and finally milled in a ball mill pot for a minimum of 24 h.

In order to improve the properties of the final product, one or more of the methods described above can be combined. Among the various possibilities, combinations of hydrothermal-hydrolysis and hydrothermal-microemulsion are most widely used [35].

Almost all of the techniques listed above allow obtaining HA with a stoichiometric ratio similar to that of bio-apatite. The most important difference with biological HA is the absence of ionic replacements that occur spontaneously within the human body [11]. In fact, natural HA contains a certain amount of ionic substitutions and impurities, such as  $Mg^{2+}$ ,  $F^-$ ,  $K^+$ ,  $Na^+$ ,  $Cl^-$  and  $Zn^{2+}$  [51].

A highly interesting line of research aims at obtaining HA products with bone-like structural organization deriving from natural templates.

Historically, the most famous example is given by coralline HA, which was first introduced in the 1970s [52]. First, the coralline template is thermally treated at 900 °C to allow the removal of all organic substances along with the decomposition of  $CaCO_3$  into CaO, while the porous microstructure of the original coral is preserved. Upon a hydrothermal process with  $(NH_4)_2HPO_4$ , conversion to  $\beta$ -tricalcium phosphate occurs and, eventually, HA is formed being the most thermodynamically stable calcium phosphate phase [53]. The use of  $KH_2PO_4$  as a mineralizer was also experimented to accelerate the ion exchange process and to avoid the formation of intermediary phases; it was also reported a better preservation of the original coralline architecture [54].

Recently, coralline HA was doped with strontium, which is known to have bone antiresorptive properties (anti-osteoporotic effect) [55].

Coral-derived HA is commercially available to surgeons in the form of porous granules for filling osseous defects, porous scaffolds for bone augmentation and spine surgery, porous plates for orbital floor repair and porous spheres used as orbital implants in enucleated patients [56].

More recently, Rattan wood has a strong similarity with bone as it exhibits a total porosity of 85 vol.% and large macropores (diameter around 250  $\mu m$ ) organized in a system of channels (mimicking the Haversian system in bone) interconnected with a network of smaller canaliculi (mimicking the Volkmann system) [57]. In this regard, Tampieri's research team developed a process of biomorphic transformation of Rattan wood in bone-like HA [58–60]. All the organic substances of wood are eliminated by pyrolysis, thus leaving behind a carbon skeleton which replicates the porous organization of the natural template. Carbonized wood is then converted to porous HA by a sequence of ion-exchange chemical reactions. A careful control of the chemical parameters of the process as well as the kinetics of the reactions is the key to allow phase transformations to faithfully occur at a molecular level. Rattan-derived biomorphic porous HA is formed by needle-like nano-sized crystals, mimicking the mineral phase of bone, and exhibits a compressive strength along the channel axis (4 MPa) comparable to that of calcified tissues [56]. In vitro investigation using MG-63 osteoblast-like cells confirmed the good biocompatibility of the wood-templated HA and in vivo tests in critical femoral defects of rats proved extensive



bone formation inside the HA channels without inflammation nor encapsulation inside connective capsule after 1 month of follow-up [61].

#### 4. Dense and Porous Hydroxyapatite

Once HA powder is produced, dense or porous HA-based products can be obtained depending on the sintering method chosen. Sintering treatment is carried out in special electric furnaces that reach high temperatures in a controlled manner, where the maximum temperature has to be properly set in order to achieve proper densification of the material [4]. The heating rate, sintering temperature and holding time depend on the material to treat; for HA, these values are in the typical ranges of 0.5–3 °C/min, 1000–1250 °C and 2–5 h, respectively [4].

As a result of the sintering process, the ceramic powders can firmly bind together, while water, carbonates and other volatile chemicals are removed in the form of gaseous products. In most cases, this causes a considerable shrinkage which has to be considered at the product design stage [4].

In order to obtain dense HA (Figure 6), sintering can be performed in several ways, including:

1. Sintering in the absence of pressure: a pressure of 60–80 MPa is used to compact the powders that are then pressurelessly sintered in air at 950–1300 °C for a few hours, with a temperature gradient of 100 °C/h. Different degree of HA density can be obtained depending on the set temperature.
2. Uniaxial hot pressing (HP): dense HA is obtained without reaching too high temperatures. This prevents the formation of other phosphates, such as tricalcium phosphate, resulting in a purer product.
3. Hot isostatic pressing (HIP): cold-pressed powders are then hot-pressed by means of the isostatic action of a gas. Very dense materials with excellent mechanical properties are obtained, which can also be further processed later.



Figure 6. Disks of dense HA (courtesy of Enrica Verné).



These three techniques allow decreasing the grain size, thus obtaining HA with quite high density, fine microstructures, high thermal stability and high mechanical properties [62].

The traditional methods to produce porous HA (Figure 7) involve the sintering of ceramic powder with specific pore-generating additives, such as naphthalene, paraffin, hydrogen peroxide or even a porous template (polymeric sponge), which burn-off at high temperatures leaving void spaces behind them [62]. Total pore volume and pore size depend on the particle size distribution of raw ceramic powder, type of fabrication techniques used, type of pore-forming agent/template and sintering conditions [63].



**Figure 7.** Examples of porous HA blocks (scaffolds) (courtesy of Enrica Verné).

The advent of additive manufacturing technologies, which provide the advantages of a relatively fast, precise, controllable and potentially scalable fabrication process, has opened new horizons in the field of porous HA and, in general, ceramic scaffolds. The potential and challenges related to 3D printing of HA and HA-based composite scaffolds have been comprehensively reviewed by Kumar et al. [64] in a recent paper.

Among the additive manufacturing technologies, lithography-based methods allow obtaining high-quality ceramic products with the best spatial resolution (less than 50  $\mu\text{m}$ ). The latest evolution of stereolithographic methods is based on digital light processing (DLP), which relies on a dynamic mask to promote the polymerization of a layer of photocurable resin containing the ceramic particles. Compared to other stereolithographic methods, this bottom-up approach carries some advantages, including the reduction of the material needed for the process and the defects introduced during the layer-wise building of the product [65]. Moreover, regardless of the shape, size and complexity of the final products, production times can be significantly decreased with obvious advantages from economic and technological viewpoints. Overall, DLP stereolithography is a highly versatile manufacturing technique with an impressive potential in improving the properties of ceramic products: in this regard, Schwentenwein et al. [66] produced bulk ceramic materials (alumina) with mechanical properties comparable to those of ceramics manufactured by traditional routes and the same group [67] employed a DLP-based multi-material approach, relying on embedding alumina/zirconia layers between outer pure alumina layers, to increase the biaxial strength to above 1 GPa (compared to 650 MPa in monolithic alumina).

In general, however, ceramic scaffolds—including the HA ones—obtained by additive manufacturing technologies typically exhibit a relatively simple porous architecture with grid-like arrangements of macro-channels (i.e., the structure of the CAD file used for printing) and, thus, do not closely replicate the trabecular architecture of cancellous bone as ceramic foams instead do. In order to overcome this limitation and further expand the potential of additive manufacturing in biomedicine, HA scaffolds were recently fabricated by DLP stereolithography using a micro-tomographic reconstruction of an open-cell polymeric foam as a CAD model [68]. As a result, truly bone-like HA scaffolds with 3D trabecular architecture, pore size, intrinsic permeability, elastic modulus and compressive strength comparable to those of human cancellous bone were obtained.

HA-based porous ceramic can develop a strong junction with natural bone as the pores allow achieving a strong mechanical interlocking with regenerating tissue, which yields a stronger fixation of the structure [61]. In general, porous HA is more resorbable and osteoconductive than dense HA. In fact, thanks to the higher surface area, more bone cells are able to attach and proliferate on the implant [63].

## 5. Mechanical Properties

From a technological viewpoint, the mechanical properties of HA-based products indeed depend on the method used for powder preparation, which determines the grain size and shape, Ca/P ratio and purity and the sintering conditions, which dictates the characteristics of microporosity [10]. If production of macroporous HA is a goal, sintering conditions and type of pore-forming agent also dictate the characteristics of macroporosity.

In general, density, grain size, compressive/torsional/flexural strength and elastic modulus increase as the sintering temperature increases. The mechanical properties of HA decrease significantly with increasing microporosity, amorphous phase and grain size. On the contrary, low porosity, high crystallinity and small grain size increase tensile strength, compressive strength, fracture toughness and stiffness. Fracture toughness can decrease due to the presence of TCP, that can form during sintering at high temperatures.

Sintered HA has superior mechanical properties as compared to cortical bone, enamel and dentin, except for fatigue strength that is quite low [10]; indeed, these properties dramatically decrease as porosity increases (Table 4). Therefore, scaffolds made of HA alone cannot be utilized for high-load-bearing applications [10] for which polymer/ceramic composites are typically preferred [69]. The polymer aims at mimicking the role of organic phase(s) in natural tissue, since the high fracture toughness and tensile strength of bone are due to the presence of collagen fibers. It is worth underlining that, upon implantation, the mechanical performance of HA scaffolds could be superior to those assessed by standard mechanical test: in fact, it was shown that fracture toughness and flexural strength of dense HA are much higher under wet conditions than in dry conditions [10].

**Table 4.** Mechanical properties of porous and dense HA and human compact bone, adapted by [10].

Material	Compressive Strength (MPa)	Tensile Strength (MPa)	Elastic Modulus (GPa)	Fracture Toughness (MPa)
Dense HA	~400	~40	~100	~1.0
Porous HA (82–86 vol.%)	0.2–0.4	-	$0.8\text{--}1.6 \times 10^{-3}$	-
Cortical bone	130–180	50–151	12–18	6–8
Cancellous bone	1–20	-	0.1–0.5	-

The use of additive manufacturing technologies allowed significantly improving the strength of HA scaffolds. For example, grid-like HA scaffolds produced by DLP stereolithography exhibited a compressive strength comparable to that of cancellous bone (1.45–1.92 MPa), although the porosity was lower (49–52 vol.%) [70]. The same fabrication method was recently combined with micro-tomographic imaging to obtain trabecular-like HA scaffolds with compressive strength of  $1.60 \pm 0.79$  MPa and bone-like porosity (80 vol.%) and permeability ( $0.75\text{--}1.74 \cdot 10^{-9}$  m<sup>2</sup>) [68]. Prolonged immersion in simulated body fluid (SBF) for up to 2 months led to no significant variation in the mechanical strength of these bone-like HA scaffolds, which can be justified by the very low dissolution rate of HA. Interestingly, these values of compressive strength are from four to eight times higher than those obtained for foam-replicated HA scaffolds with analogous porosity (Table 4). Another study revealed that using nano-sized HA particles (diameter around 150 nm) to coat the polyurethane sponge in the foam-replica method yielded just minor improvement in the compressive strength (0.51 MPa) [71]. This suggests that the scaffold production method plays a major role over the particle size in affecting the mechanical performance of the final macroporous product.

## 6. Applications of HA in Tissue Engineering

In 1969, Levitt et al. [72] wrote one of the first scientific papers on the possible applications of HA to make complex implants in contact with bone to repair and regenerate hard tissues, thus figuring out the use of HA in BTE.

HA powders are mainly used to produce coatings on metallic implants, as starting material for making scaffolds, or as fillers for polymer-matrix composites [73].

HA powders as coatings began to be used mainly in the late 1980s; more specifically, Furlong and Osborn [74] were the first to begin studying HA coatings for clinical applications and, since then, these coatings have shown good results with a 2% failure rate for a 10-year follow-up study. In this way, the use of CaPs has somewhat expanded even in the field of load-bearing applications, as metal substrates help to increase the poor mechanical strength of ceramics [12,25].

Usually, HA coatings are applied on metallic implants by plasma treatment; clinical results reveal that HA-coated implants have a longer lifetime as compared to uncoated implants, which can be very beneficial especially for younger patients. Thanks to the presence of HA, bone tissue can better integrate with the implant (osteoconduction) and, in addition, HA reduces the release of metal ions from the implant, thus avoiding undesirable inflammatory reactions or toxic effects [62].

In order to achieve positive results, it is crucial to choose the right thickness of the coating to obtain satisfactory adhesion and interfacial stability; it has been shown that good outcomes are obtained with a thickness in the range of 40 to 200  $\mu\text{m}$  [62].

An important use of porous HA is for the controlled drug release in bone disorders such as bone tumors or osteoporosis. Porous HA granules or scaffolds loaded with drugs ensures a localized and prolonged release of drugs, which speeds bone healing [62]. A recent study by Ferreira-Ermita et al. [75] showed in a rabbit model that HA associated with magnetite nanoparticles was an effective platform for the release of ciprofloxacin in the treatment of osteomyelitis.

Custom-made porous HA scaffolds are also widely used as gap filler to treat bone defects through promoting bone ingrowth, especially in cases where conventional techniques have failed. For example, Quarto et al. [76] implanted HA scaffolds seeded with *in vitro* expanded autologous bone marrow cells to cure large bone diseases (4–7 cm) of the ulna, humerus and tibia in patients of different ages. In another study, Vacanti et al. [77] proposed a natural coral-derived implant (porous HA; pore size 500  $\mu\text{m}$ , ProOsteon) functionalized *in vitro* with autologous periosteal cells to treat a traumatic avulsion of the distal phalanx of a man thumb. Following a similar approach, Morishita et al. [78] treated a disease due to tumors in a tibia and in a femur by using HA scaffolds seeded with *in vitro* expanded autologous bone marrow stromal cells.

For the preparation of 3D scaffolds, HA can be used alone or in combination with different polymers such as poly(lactic-co-glycolic) acid (PLGA), poly(L-lactic acid) (PLLA) and polycaprolactone (PCL) to improve the mechanical properties or impart a controllable resorbability [79].

Ignjatovic et al. [80] and Wang et al. [81] fabricated HA/PLLA and HA/polyethylene composites, respectively, and in both cases these composites had a sufficient mechanical strength to be utilized in BTE. HA/polyethylene composites are also commercialized under the tradename of HAPEX and clinically used for the replacement of middle ear bones and orbital floor repair. A comprehensive picture of the latest advances in HA/polymer composites and cell-seeded HA constructs has been recently reported by Kattimai et al. [82].

The application of bone synthetic grafts has further evolved in BTE thanks to improvement of different additive manufacturing techniques, including selective laser sintering, laser cladding, 3D printing and stereolithography [64]. Various combinations of HA with other materials, including polymers, bioactive glasses and other crystalline ceramics, are also possible through multi-material printing to obtain composites; this approach has been typically limited to robocasting techniques, but recent stereolithographic systems have also been adapted to process more than one ceramic material simultaneously (alumina and zirconia in early trials) [67].

Surgeons often prefer injectable biomaterials as compared to rigid scaffolds, as the pastes are easy to handle and conform to the anatomy of the osseous defect. In this regard, there are many commercially-available CaP-based cements that form a workable paste after being mixed with an aqueous saline solution [83]. This putty can be easily shaped during surgery to perfectly match the geometry of the bone defect prior to set within 10–20 min. Upon setting, the reactants reprecipitate until the entire material is converted to finely porous HA. After being implanted *in vivo*, CaP cements are gradually resorbed over time and replaced with newly-formed bone.

Mixing with collagen was apparently regarded as a good strategy to improve the biomimetic properties of bone cements. In this regard, Cuzmar et al. [84] analyzed the osteogenic capacity of Ca-deficient HA microspheres with or without collagen obtained by emulsification of a CaP cement paste and compared the performance with an injectable ceramic cement having the same composition. After implantation in femur condyles of rabbits, histological analysis revealed that the cements presented cellular activity only in the margins of the material, whereas the microspheres were well coated with osteogenic cells. As a result, bone ingrowth was enhanced by the microspheres, with a tenfold increase as compared to the conventional cement, which was associated to the higher accessibility for the cells provided by the macroporous network between the microspheres and the larger surface area available for osteoconduction. Interestingly, no significant differences were found in terms of bone formation associated with the presence of collagen in the microspheres, although a more extensive resorption of the collagen-containing material was observed.

Some examples of commercially-available HA products for osseous repair and BTE are also listed in Table 5.

**Table 5.** Various examples of commercially-available HA products for BTE, adapted from [73].

Tradename	Producer	Country
Actifuse	ApaTech	UK
ApaPore	ApaTech	UK
Apaceram	Pentax	Japan
Bonefil	Pentax	Japan
Bonetite	Pentax	Japan
Bonoceram	Sumitomo Osaka Cement	Japan
Bioroc	Depuy—Bioland	France
Cerapatite	Ceraver	France
BoneSource	Stryker Orthopaedics	NJ, USA
Calcitite	Zimmer	IN, USA
Osteograft	Ceramed	CO, USA

Although being mainly employed for the repair of bone defects, HA has also been recently proposed in some emerging applications in contact with soft tissues, including ophthalmology, wound regeneration and anticancer therapies; a comprehensive picture of these novel research topics has been recently provided by Kargozar et al. [85]. As regards ocular applications, HA is marketed and clinically used since the 1980s in the form of porous orbital implants for enucleation (e.g., coralline or synthetic HA spheres) [86].

## 7. Conclusions

Considering all the various biomaterials currently available in bone regenerative strategies, calcium phosphates (CaPs) and, specifically, hydroxyapatite (HA), are among the most commonly-used due to their compositional and structural similarities to natural bone and teeth, as well as exceptional biocompatibility and biological behavior in contact with body fluids, which make them materials of choice for producing synthetic bone grafts to be used as an alternative to transplantation (auto- and allografts).

Due to an excellent osteoconductive potential, HA has been highly favored in bone BTE applications, being the main representative of commercial products currently used in clinical practice. Several studies demonstrated the capability of HA to create a favorable environment for promoting new bone tissue ingrowth and regeneration, resulting in a perfect integration of the graft without leading to the development of a severe immune response. These appealing properties made it an optimal candidate in different clinical fields. To date, the main biomedical applications of HA include osseous defect filling (e.g., augmentation and stabilization of the jawbone in maxillofacial reconstruction), spinal fusion, bone filling after tumor operation, replacement of middle ear bones and repair of orbital floor fractures. Great results were also achieved in the development of drug delivery systems and carriers of bioactive peptides and/or various cell types.

In recent years, the growing interest in three-dimensional (3D), *in vivo*-like bone tissue engineering approaches made the biomedical research focus on the development of HA porous grafts mimicking the trabecular architecture of human spongy bone. In this regard, the main challenge to be addressed in the future is certainly represented by the need to achieve adequate mechanical properties to allow a safe use of the graft. Like all ceramic materials, in fact, HA has low tensile strength and an intrinsic brittleness that limits its application in load-bearing anatomical sites. Currently, the most common strategy to overcome this drawback is represented by the production of polymer/ceramic composite scaffolds, which have been directly inspired by the peculiar compositional features of biological bone, where the presence of collagen fibers confers high fracture toughness and tensile strength to the tissue. Looking at the future, there is a great expectation in the use of additive manufacturing technologies combined with computer aided design (CAD) and physical simulation tools, with the ambitious aim of introducing the use of advanced tailored—and even personalized—BTE products in clinical practice.



**Author Contributions:** All the authors equally contributed to the present work. All authors have read and agreed to the published version of the manuscript.

**Funding:** This research received no external funding.

**Institutional Review Board Statement:** Not applicable.

**Informed Consent Statement:** Not applicable.

**Data Availability Statement:** The data reported in this work, being a review paper, can be found in the original sources cited in the reference list.

**Conflicts of Interest:** The authors declare no conflict of interest.

## References

1. Albee, F.H.; Morrison, H.F. Studies in bone growth triple calcium phosphate as a stimulus to osteogenesis. *Ann. Surg.* **1920**, *71*, 32–39.
2. Jazayeri, H.E.; Rodriguez-Romero, M.; Razavi, M.; Tahiri, M.; Ganjawalla, K.; Rasoulianboroujeni, M.; Malekshoaraie, M.H.; Khoshroo, K.; Tayebi, L. The cross-disciplinary emergence of 3D printed bioceramic scaffolds in orthopedic bioengineering. *Ceram. Int.* **2018**, *44*, 1–9. [[CrossRef](#)]
3. Jeong, J.; Kim, J.H.; Shim, J.H.; Hwang, N.S.; Heo, C.Y. Bioactive calcium phosphate materials and applications in bone regeneration. *Biomater. Res.* **2019**, *23*, 4. [[CrossRef](#)]
4. Dorozhkin, S.V. Calcium orthophosphate bioceramics. *Ceram. Int.* **2015**, *41*, 13913–13966. [[CrossRef](#)]
5. Eliaz, N.; Metoki, N. Calcium Phosphate Bioceramics: A Review of Their History, Structure, Properties, coating Technologies and Biomedical Applications. *Materials* **2017**, *10*, 334. [[CrossRef](#)] [[PubMed](#)]
6. Dorozhkin, S.V. Calcium orthophosphates as bioceramics: State of the art. *J. Funct. Biomater.* **2010**, *1*, 22–107. [[CrossRef](#)]
7. Dorozhkin, S.V. Multiphasic calcium orthophosphate (CaPO<sub>4</sub>) bioceramics and their biomedical applications. *Ceram. Int.* **2016**, *42*, 6529–6554. [[CrossRef](#)]
8. Carvalho, B.; De Rompen, E.; Lecloux, G.; Schupbach, P.; Dory, E. Effect of sintering on in vivo biological performance of bovine hydroxyapatite. *Materials* **2019**, *12*, 3946. [[CrossRef](#)] [[PubMed](#)]
9. Mohamad Yunos, D.; Bretcanu, O.; Boccaccini, A.R. Polymer-bioceramic composites for tissue engineering scaffolds. *J. Mater. Sci.* **2008**, *43*, 4433–4442. [[CrossRef](#)]
10. Rezwan, K.; Chen, Q.Z.; Blaker, J.J.; Boccaccini, A.R. Biodegradable and bioactive porous polymer/inorganic composite scaffolds for bone tissue engineering. *Biomaterials* **2006**, *27*, 3413–3431. [[CrossRef](#)] [[PubMed](#)]
11. Owen, R.G.; Dard, M.; Larjava, H. Hydroxyapatite/beta-tricalcium phosphate biphasic ceramics as regenerative material for the repair of complex bone defects. *J. Biomed. Mater. Res. B Appl. Biomater.* **2018**, *106*, 2493–2512. [[CrossRef](#)]
12. Søballe, K. Hydroxyapatite ceramic coating for bone implant fixation: Mechanical and histological studies in dogs. *Acta Orthop. Scand.* **1993**, *64*, 1–58. [[CrossRef](#)]
13. Fiume, E.; Barberi, J.; Verné, E.; Baino, F. Bioactive Glasses: From Parent 45S5 Composition to Scaffold-Assisted Tissue-Healing Therapies. *J. Funct. Biomater.* **2018**, *9*, 24. [[CrossRef](#)]
14. Cao, W.; Hench, L.L. Bioactive materials. *Ceram. Int.* **1996**, *22*, 493–507. [[CrossRef](#)]
15. Horowitz, R.A.; Mazor, Z.; Foitzik, C.; Prasad, H.; Rohrer, M.; Palti, A.  $\beta$ -Tricalcium Phosphate As Bone Substitute Material. *J. Osseointegr.* **2010**, *1*, 60–68.
16. Islam, M.T.; Felfel, R.M.; Abou Neel, E.A.; Grant, D.M.; Ahmed, I.; Hossain, K.M.Z. Bioactive calcium phosphate-based glasses and ceramics and their biomedical applications: A review. *J. Tissue Eng.* **2017**, *8*, 2041731417719170. [[CrossRef](#)] [[PubMed](#)]
17. Ebrahimi, M.; Botelho, M.G.; Dorozhkin, S.V. Biphasic calcium phosphates bioceramics (HA/TCP): Concept, physico-chemical properties and the impact of standardization of study protocols in biomaterials research. *Mater. Sci. Eng. C* **2017**, *71*, 1293–1312. [[CrossRef](#)]
18. Habraken, W.J.E.M.; Tao, J.; Brylka, L.J.; Friedrich, H.; Bertinetti, L.; Schenk, A.; Verch, A.; Dmitrovic, V.; Bomans, P.H.H.; Frederik, P.M.; et al. Ion-association complexes unite classical and non-classical theories for the biomimetic nucleation of calcium phosphate. *Nat. Commun.* **2013**, *4*, 1507. [[CrossRef](#)] [[PubMed](#)]
19. Kumta, P.N.; Sfeir, C.; Lee, D.H.; Olton, D.; Choi, D. Nanostructured calcium phosphates for biomedical applications: Novel synthesis and characterization. *Acta Biomater.* **2005**, *1*, 65–83. [[CrossRef](#)] [[PubMed](#)]
20. Lawson, A.C.; Czernuszka, J.T. Collagen-calcium phosphate composites. *Proc. Inst. Mech. Eng. H* **1998**, *212*, 413–425. [[CrossRef](#)] [[PubMed](#)]
21. Albuлесcu, R.; Popa, A.-C.; Enciu, A.-M.; Albuлесcu, L.; Dudau, M.; Popescu, I.D.; Mihai, S.; Codrici, E.; Pop, S.; Lupu, A.-R.; et al. Comprehensive In Vitro Testing of Calcium Phosphate-Based Bioceramics with Orthopedic and Dentistry Applications. *Materials* **2019**, *10*, 3704. [[CrossRef](#)] [[PubMed](#)]
22. Szczeń, A.; Hołysz, L.; Chibowski, E. Synthesis of hydroxyapatite for biomedical applications. *Adv. Colloid Interface Sci.* **2017**, *249*, 321–330. [[CrossRef](#)] [[PubMed](#)]
23. Wopenka, B.; Pasteris, J.D. A mineralogical perspective on the apatite in bone. *Mater. Sci. Eng. C* **2005**, *25*, 131–143. [[CrossRef](#)]



24. Astala, R.; Stott, M.J. First principles investigation of mineral component of bone: CO<sub>3</sub> substitutions in hydroxyapatite. *Chem. Mater.* **2005**, *17*, 4125–4133. [[CrossRef](#)]
25. Best, S.M.; Porter, A.E.; Thian, E.S.; Huang, J. Bioceramics: Past, present and for the future. *J. Eur. Ceram. Soc.* **2008**, *28*, 1319–1327. [[CrossRef](#)]
26. Rivera-Muñoz, E.M. Hydroxyapatite-Based Materials: Synthesis and Characterization. In *Biomedical Engineering: Frontiers and Challenges*; Fazel-Rezai, R., Ed.; Intech Open: Rijeka, Croatia, 2011.
27. Doi, Y.; Shibutani, T.; Moriwaki, Y.; Kajimoto, T.; Iwayama, Y. Sintered carbonate apatites as bioresorbable bone substitutes. *J. Biomed. Mater. Res.* **1998**, *39*, 603–610. [[CrossRef](#)]
28. Rahyussalim, A.J.; Supriadi, S.; Marsetio, A.F.; Pribadi, P.M.; Suharno, B. The potential of carbonate apatite as an alternative bone substitute material. *Med. J. Indones.* **2019**, *28*, 92–97. [[CrossRef](#)]
29. Wang, A.N.; Wu, L.G.; Li, X.L.; Sun, Y.D.; Wang, J.; Wang, S.W.; Jia, A.X.; Wang, C.; Zhang, Y.Y.; Fu, Q.Q.; et al. Study on the Blend Film Prepared by Chitosan and Gelatin. *Adv. Mater. Res.* **2011**, *201–203*, 2866–2869. [[CrossRef](#)]
30. Bhattacharjee, A.; Fang, Y.; Hooper, T.J.N.; Kelly, N.L.; Gupta, D.; Balani, K.; Manna, I.; Baikie, T.; Bishop, P.T.; White, T.J.; et al. Crystal chemistry and antibacterial properties of cupriferous hydroxyapatite. *Materials* **2019**, *12*, 1814. [[CrossRef](#)]
31. López-Noriega, A.; Arcos, D.; Izquierdo-Barba, I.; Sakamoto, Y.; Terasaki, O.; Vallet-Regí, M. Ordered mesoporous bioactive glasses for bone tissue regeneration. *Chem. Mater.* **2006**, *18*, 3137–3144. [[CrossRef](#)]
32. Baino, F.; Fiume, E.; Miola, M.; Leone, F.; Onida, B.; Verné, E. Fe-doped bioactive glass-derived scaffolds produced by sol-gel foaming. *Mater. Lett.* **2019**, *235*, 207–211. [[CrossRef](#)]
33. Fiume, E.; Serino, G.; Bignardi, C.; Verné, E.; Baino, F. Bread-derived bioactive porous scaffolds: An innovative and sustainable approach to bone tissue engineering. *Molecules* **2019**, *24*, 2954. [[CrossRef](#)] [[PubMed](#)]
34. Silva, C.; Pinheiro, A.; De Oliveira, R.; Goes, J.C.; Aranha, N.; De Oliveira, L.; Sombra, A. Properties and in vivo investigation of nanocrystalline hydroxyapatite obtained by mechanical alloying. *Mater. Sci. Eng. C* **2004**, *24*, 549–554. [[CrossRef](#)]
35. Sadat-Shojai, M.; Khorasani, M.T.; Dinpanah-Khoshdargi, E.; Jamshidi, A. Synthesis methods for nanosized hydroxyapatite with diverse structures. *Acta Biomater.* **2013**, *9*, 7591–7621. [[CrossRef](#)] [[PubMed](#)]
36. Roy, M.; Bandyopadhyay, A.; Bose, S. Chapter 6: Ceramics in Bone Grafts and Coated Implants. In *Materials for Bone Disorders*; Bose, S., Bandyopadhyay, A., Eds.; Academic Press (Elsevier): London, UK, 2017; pp. 265–314.
37. Li, B.; Webster, T. *Orthopedic Biomaterials: Advances and Applications*; Springer: Cham, Switzerland, 2017.
38. Nasiri-Tabrizi, B.; Honarmandi, P.; Ebrahimi-Kahrizangi, R. Synthesis of nanosize single-crystal hydroxyapatite via mechanochemical method. *Mater. Lett.* **2009**, *63*, 543–546. [[CrossRef](#)]
39. Zhan, J.; Tseng, Y.H.; Chan, J.C.C.; Mou, C.Y. Biomimetic formation of hydroxyapatite nanorods by a single-crystal-to-single-crystal transformation. *Adv. Funct. Mater.* **2005**, *15*, 2005–2010. [[CrossRef](#)]
40. Tenhuisen, K.S.; Brown, P.W. Formation of calcium-deficient hydroxyapatite from  $\alpha$ -tricalcium phosphate. *Biomaterials* **1998**, *19*, 2209–2217. [[CrossRef](#)]
41. Park, H.C.; Baek, D.J.; Park, Y.M.; Yoon, S.Y.; Stevens, R. Thermal stability of hydroxyapatite whiskers derived from the hydrolysis of  $\alpha$ -TCP. *J. Mater. Sci.* **2004**, *39*, 2531–2534. [[CrossRef](#)]
42. Fathi, M.; Hanifi, A.; Mortazavi, V. Preparation and bioactivity evaluation of bone-like hydroxyapatite nanopowder. *J. Mater. Process. Technol.* **2008**, *202*, 536–542. [[CrossRef](#)]
43. Sopyan, I.; Singh, R.; Hamdi, M. Synthesis of nano sized hydroxyapatite powder using sol-gel technique and its conversion to dense and porous bodies. *Indian J. Chem. A* **2008**, *47*, 1626–1631.
44. Zhu, R.; Yu, R.; Yao, J.; Wang, D.; Ke, J. Morphology control of hydroxyapatite through hydrothermal process. *J. Alloys Compd.* **2008**, *457*, 555–559. [[CrossRef](#)]
45. Chun, H.J.; Park, K.; Kim, C.-H.; Khang, G. *Novel Biomaterials for Regenerative Medicine*, 1st ed.; Springer: Singapore, 2018.
46. Guo, G.; Sun, Y.; Wang, Z.; Guo, H. Preparation of hydroxyapatite nanoparticles by reverse microemulsion. *Ceram. Int.* **2005**, *31*, 869–872. [[CrossRef](#)]
47. Sun, Y.; Guo, G.; Wang, Z.; Guo, H. Synthesis of single-crystal HAP nanorods. *Ceram. Int.* **2006**, *32*, 951–954. [[CrossRef](#)]
48. Li, H.; Zhu, M.Y.; Li, L.H.; Zhou, C.R. Processing of nanocrystalline hydroxyapatite particles via reverse microemulsions. *J. Mater. Sci.* **2008**, *43*, 384–389. [[CrossRef](#)]
49. Hazar Yoruç, A.B.; Ipek, Y. Sonochemical synthesis of hydroxyapatite nanoparticles with different precursor reagents. *Acta Phys. Pol. A* **2012**, *121*, 230–232. [[CrossRef](#)]
50. Ruksudjarit, A.; Pengpat, K.; Rujijanagul, G.; Tunkasiri, T. Synthesis and characterization of nanocrystalline hydroxyapatite from natural bovine bone. *Curr. Appl. Phys.* **2008**, *8*, 270–272. [[CrossRef](#)]
51. Qu, H.; Fu, H.; Han, Z.; Sun, Y. Biomaterials for bone tissue engineering scaffolds: A review. *RSC Adv.* **2019**, *9*, 26252–26262. [[CrossRef](#)]
52. White, R.A.; Weber, J.N.; White, E.W. Replamineform: A New Process for Preparing Porous Ceramic, Metal, and Polymer Prosthetic Materials. *Science* **1972**, *176*, 922–924. [[CrossRef](#)]
53. White, E.W.; Weber, J.N.; Roy, D.M.; Owen, E.L.; Chiroff, R.T.; White, R.A. Replamineform Porous Biomaterials for Hard Tissue Implant Applications. *J. Biomed. Mater. Res.* **1975**, *6*, 23–27. [[CrossRef](#)]
54. Xu, Y.; Wang, D.; Yang, L.; Tang, H. Hydrothermal Conversion of Coral into Hydroxyapatite. *Mater. Charact.* **2001**, *47*, 83–87. [[CrossRef](#)]

55. Liu, W.; Wang, T.; Shen, Y.; Pan, H.; Peng, S.; Lu, W.W. Strontium Incorporated Coralline Hydroxyapatite for Engineering Bone. *ISRN Biomater.* **2013**, *2013*, 649163. [[CrossRef](#)]
56. Damien, E.; Revell, P.A. Coralline Hydroxyapatite Bone Graft Substitute: A Review of Experimental Studies and Biomedical Applications. *J. Appl. Biomater. Biomech.* **2004**, *2*, 65–73. [[PubMed](#)]
57. Tampieri, A.; Sprio, S.; Ruffini, A.; Celotti, G.; Lesci, I.G.; Roveri, N. From Wood to Bone: Multi-Step Process to Convert Wood Hierarchical Structures into Biomimetic Hydroxyapatite Scaffolds for Bone Tissue Engineering. *J. Mater. Chem.* **2009**, *19*, 4973–4980. [[CrossRef](#)]
58. Ruffini, A.; Sprio, S.; Tampieri, A. Wood Structures with Organized Morphology for Bone Substitutes. *J. Appl. Biomater. Biomech.* **2007**, *5*, 207.
59. Sprio, S.; Ruffini, A.; Valentini, F.; D’Alessandro, T.; Sandri, M.; Panseri, S.; Tampieri, A. Biomimesis and Biomorphic Transformations: New Concepts Applied to Bone Regeneration. *J. Biotechnol.* **2011**, *156*, 347–355. [[CrossRef](#)]
60. Ruffini, A.; Sprio, S.; Tampieri, A. Study of the Hydrothermal Transformation of Wood-Derived Calcium Carbonate into 3D Hierarchically Organized Hydroxyapatite. *Chem. Eng. J.* **2013**, *217*, 150–158. [[CrossRef](#)]
61. Ruffini, A.; Sprio, S.; Tampieri, A. Towards Hierarchically Organized Scaffolds for Bone Substitutes from Wood Structures. *Key Eng. Mater.* **2008**, *361–363*, 959–962.
62. Suchanek, W.; Yoshimura, M. Processing and properties of hydroxyapatite-based biomaterials for use as hard tissue re-placement implants. *J. Mater. Res.* **1998**, *13*, 94–117. [[CrossRef](#)]
63. Al-Naib, U.M.B. Introductory chapter: A Brief Introduction to Porous Ceramic. In *Recent Advances in Porous Ceramics*; Al-Naib, U.M.B., Ed.; Intech Open: Rijeka, Croatia, 2018.
64. Kumar, A.; Kargozar, S.; Baino, F.; Han, S.S. Additive Manufacturing Methods for Producing Hydroxyapatite and Hydroxyapatite-Based Composite Scaffolds: A Review. *Front. Mater.* **2019**, *6*, 313. [[CrossRef](#)]
65. Potestio, I. Lithoz: How lithography-based ceramic AM is expanding the opportunities for technical ceramics. *Powder Inject. Mould. Int.* **2019**, *13*, 2–5.
66. Schwentenwein, M.; Homa, J. Additive manufacturing of dense alumina ceramics. *Int. J. Appl. Ceram. Technol.* **2015**, *12*, 1–7. [[CrossRef](#)]
67. Schlacher, J.; Hofer, A.-K.; Geier, S.; Kraveva, I.; Papšik, R.; Schwentenwein, M.; Bermejo, R. Additive manufacturing of high-strength alumina through a multi-material approach. *Open Ceram.* **2021**, *5*, 100082. [[CrossRef](#)]
68. Baino, F.; Magnaterra, G.; Fiume, E.; Schiavi, A.; Tofan, L.; Schwentenwein, M.; Verné, E. Digital light processing stereolithography of hydroxyapatite scaffolds with bone-like architecture, permeability, and mechanical properties. *J. Am. Ceram. Soc.* **2021**, 1–10. [[CrossRef](#)]
69. Tanner, K.E. Bioactive ceramic-reinforced composites for bone augmentation. *J. R. Soc. Interface* **2012**, *7*, S541–S557. [[CrossRef](#)]
70. Feng, C.; Zang, K.; He, R.; Ding, G.; Xia, M. Additive manufacturing of hydroxyapatite bioceramic scaffolds: Dispersion, digital light processing, sintering, mechanical properties, and biocompatibility. *J. Adv. Ceram.* **2020**, *9*, 360–373. [[CrossRef](#)]
71. Gervaso, F.; Scalera, F.; Kunjalukkal Padmanabhan, S.; Sannino, A.; Licciulli, A. High performance hydroxyapatite scaffolds for bone tissue engineering applications. *Int. J. Appl. Ceram. Technol.* **2012**, *9*, 507–516. [[CrossRef](#)]
72. Levitt, G.E.; Crayton, P.H.; Monroe, E.A.; Condrate, R.A. Forming methods for apatite prosthesis. *J. Biomed. Mater. Res.* **1969**, *3*, 683–685. [[CrossRef](#)]
73. Dorozhkin, S. Medical Application of Calcium Orthophosphate Bioceramics. *BIO* **2011**, *1*, 1–51. [[CrossRef](#)]
74. Furlong, R.J.; Osborn, J.F. Fixation of hip prostheses by hydroxyapatite ceramic coatings. *J. Bone Jt. Surg.* **1991**, *73*, 741–745. [[CrossRef](#)]
75. Ferreira-Ermita, D.A.; Valente, F.L.; Carlo-Reis, E.C.; Araújo, F.R.; Ribeiro, I.M.; Cintra, C.C.; Borges, A.P. Characterization and in vivo biocompatibility analysis of synthetic hydroxyapatite compounds associated with magnetite nanoparticles for a drug delivery system in osteomyelitis treatment. *Results Mater.* **2020**, *5*, 100063. [[CrossRef](#)]
76. Quarto, R.; Mastrogiacomo, M.; Cancedda, R.; Kutepov, S.M.; Mukhachev, V.; Lavroukov, A.; Kon, E.; Marcacci, M. Repair of large bone defects with the use of autologous bone marrow stromal cells. *N. Engl. J. Med.* **2001**, *344*, 385–386. [[CrossRef](#)] [[PubMed](#)]
77. Vacanti, C.A.; Bonassar, L.J.; Vacanti, M.P.; Shufflebarger, J. Replacement of an Avulsed Phalanx with Tissue-Engineered Bone. *N. Engl. J. Med.* **2001**, *344*, 1511–1514. [[CrossRef](#)] [[PubMed](#)]
78. Morishita, T.; Honoki, K.; Ohgushi, H.; Kotobuki, N.; Matsushima, A.; Takakura, Y. Tissue engineering approach to the treatment of bone tumors: Three cases of cultured bone grafts de-rived from patients’ mesenchymal stem cells. *Artif. Organs* **2006**, *30*, 115–118. [[CrossRef](#)] [[PubMed](#)]
79. Haider, A.; Haider, S.; Han, S.S.; Kang, I.K. Recent advances in the synthesis, functionalization and biomedical applications of hydroxyapatite: A review. *RSC Adv.* **2017**, *7*, 7442–7458. [[CrossRef](#)]
80. Ignjatovic, N.; Savic, V.; Najman, S.; Plavsic, M.; Uskokovic, D. A study of HAp/PLLA composite as a substitute for bone powder. *Biomaterials* **2001**, *22*, 571–575. [[CrossRef](#)]
81. Wang, M.; Joseph, R.; Bonfield, W. Hydroxyapatite-polyethylene composites for bone substitution: Effects of ceramic particle size and morphology. *Biomaterials* **1998**, *19*, 2357–2366. [[CrossRef](#)]
82. Kattimani, V.S.; Kondaka, S.; Lingamaneni, K.P. Hydroxyapatite—Past, Present, and Future in Bone Regeneration. *Bone Tissue Regen. Insights* **2016**, *7*, 9–19. [[CrossRef](#)]

83. Baino, F. Ceramics for bone replacement: Commercial products and clinical use. In *Advances in Ceramic Biomaterials*; Palmero, P., Cambier, F., De Barra Editors, E., Eds.; Woodhead Publishing (Elsevier): Cambridge, UK, 2017; pp. 249–278.
84. Cuzmar, E.; Perez, R.A.; Manzanares, M.-C.; Ginebra, M.-P.; Franch, J. In Vivo Osteogenic Potential of Biomimetic Hydroxyapatite/Collagen Microspheres: Comparison with Injectable Cement Pastes. *PLoS ONE* **2015**, *10*, e0131188.
85. Kargozar, S.; Singh, R.K.; Kim, H.W.; Baino, F. “Hard” ceramics for “Soft” tissue engineering: Paradox or opportunity? *Acta Biomater.* **2020**, *115*, 1–28. [[CrossRef](#)]
86. Baino, F.; Vitale-Brovarone, C. Ceramics for oculo-orbital surgery. *Ceram. Int.* **2015**, *41*, 5213–5231. [[CrossRef](#)]